

Contents lists available at ScienceDirect

Fuel

journal homepage: www.elsevier.com/locate/fuel

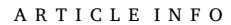


Full Length Article

Direct conversion of toluene into styrene with high selectivity over a composite catalyst

Qijun Yu^{a,b}, Jinzhe Li^a, Changcheng Wei^{a,b}, Zhongmin Liu^{a,b,*}

- ^a National Engineering Laboratory for Methanol to Olefins, Dalian National Laboratory for Clean Energy, Dalian Institute of Chemical Physics, Chinese Academy of Sciences, Dalian 116023, China
- b University of Chinese Academy of Sciences, Beijing 100049, China



Keywords:
Toluene
Side-chain alkylation
X zeolite
Sodium borate
C-H bond activation

ABSTRACT

Although side-chain methylation of toluene with methanol to produce styrene has been investigated in the past decades, commercial application of this process is still a great challenge due to the lack of efficient catalysts. Here we present a bifunctional catalyst composed of dehydrated sodium borate (Na₂B₄O₇) and zeolite (CsX) that yields a high selectivity to styrene (89.6%) with a relative high toluene conversion (9.57%). Na₂B₄O₇ not only contributes to the formation of the reaction intermediate formaldehyde but also constructs the frustrated Lewis pairs (FLPs) with basic sites on the zeolites, which could activate C–H bond in the methyl group of toluene more efficiently. Thus, the crucial role of boron species is revisited. The nature of cesium in CsX is found to be important for the reactivity of the bifunctional catalyst. Good reaction performance on composite catalyst Na₂B₄O₇-CsX also depends on the spatial proximity and mass ratio of the two components.

1. Introduction

Compared with the conventional two-step route to styrene, typically through the reaction of benzene with ethylene and sequential dehydrogenation of ethylbenzene, the coupling reaction of toluene with methanol opens a new route to produce styrene which is a significant raw material for polystyrene, acrylonitrile-styrene resin and styrene-butadiene rubber [1,2]. In spite of many researches devoted to this reaction in the past decades, commercial application is not yet implemented due to the lack of efficient catalysts.

The concept of Lewis acid-base synergistic catalysis is widely accepted for this reaction [3–5]. The base sites activate the methyl group of toluene to form benzyl carbon anion and dehydrogenate methanol to formaldehyde which is considered as true alkylating reagent [6,7]; the Lewis acid sites adsorb and stabilize toluene. The base strengthen is crucial for this reaction [8]. The active intermediate HCHO could decompose into CO and H_2 on strong base sites [9], and yet, when basicity is too weak, the methyl side chain of toluene becomes difficult to be activated.

Alkali ion-exchanged Al-rich X zeolites are the most representative catalysts for converting toluene to styrene. The alkali cations serve as Lewis acids and the oxygen atoms of zeolite skeleton with partial

negative charge act as Lewis bases. Moreover, the higher the atomic number of alkali cations balancing negative charge of zeolite framework, the stronger the basicity of zeolite, functioning in the order: ${\rm Li}^+<{\rm Na}^+<{\rm K}^+<{\rm Rb}^+<{\rm Cs}^+$ [10,11]. Among these catalysts, Cs-exchanged X (CsX) zeolite shows superior catalytic activities because of not only its effective base strength associated with Lewis acids but also zeolite's supercage with 12-member ring pore openings which allow for the facile diffusion and adsorption of toluene [3,12,13]. Therefore, CsX as well as the post-modification on it have been widely concerned.

It is also commonly accepted that formaldehyde originating from dehydrogenation of methanol is true alkylating reagent which would react with toluene through aldol-like condensation mechanism [3,6,7]. Therefore, addition of second component that could contribute to dehydrogenation of methanol to formaldehyde into CsX would increase catalytic activity. Balkrishna B. Tope *et al.* found that mechanical mixing of CsX with metal borates promoted the catalytic reactivity due to the added metal borates facilitating the formaldehyde formation [14]. The similar results were reported by Hideshi Hattori *et al.* using ZnO as an effective additive [15]. The direct side chain methylation of toluene with HCHO was also carried out by Hoin Lee *et al.* [16]. In their work, trioxane was adopted for in situ generating formaldehyde on H₃PO₄/SiO₂ catalyst, with which both toluene conversion and the yield of side-

E-mail address: liuzm@dicp.ac.cn (Z. Liu).



^{*} Corresponding author at: National Engineering Laboratory for Methanol to Olefins, Dalian National Laboratory for Clean Energy, Dalian Institute of Chemical Physics, Chinese Academy of Sciences, Dalian 116023, China.

chain products were enhanced. However, the catalyst suffers from quick deactivation due to high concentration of HCHO [16]. Qiao Han et~al. modified CsX with various dehydrogenation catalysts and found that sodium borate (Na₂B₄O₇) and CuO/SiO₂ were more effective, but no detailed mechanistic explanation was elaborated [17]. In addition, boron-modified CsX zeolites were proved the most effective catalytic systems to date, even though the role of boron species was not clearly elucidated [18,19].

In the present work, a series of methanol dehydrogenation catalysts as well as h-BN were physically mixed with CsX. These introduced second components could effectively enhance the alkylation reactivity. $Na_2B_4O_7$ was found to be most effective additive for styrene production. Besides, a possible mechanistic pathway was put forward to reveal why $Na_2B_4O_7$ is superior to any other additives. This mechanism might also be applied to other boron additive moderately.

2. Experimental

2.1. Catalyst preparation

NaX zeolite (from Nankai catalysts company with Si/Al of 1.18 and Na content of 12.03 wt%) was ion-exchanged to prepare CsX. CsX-a was prepared by conventional ion exchange procedure: 30 g NaX was ion-exchanged two times in aqueous solution of cesium hydroxide (0.4 mol/L) at 80 °C for 2 h per time (liquid/solid ratio: 5 ml/1 g). The slurries were filtered under negative pressure and washed with excess distilled water. The obtained materials were dried at 100 °C overnight and calcined at 540 °C in air for 3 h.

The sample CsX-b was obtained as follows: 30 g NaX was ion-exchanged three times with 0.4 mol/L cesium hydroxide aqueous solution at 80 °C (liquid/solid ratio, 5 ml/1 g) for 2 h per time. The obtained materials were dried at 100 °C overnight and calcined in air at 540 °C for 3 h. Then, the calcined material was ion-exchanged with dilute aqueous solution of sodium nitrate (about 0.01 mol/L) again at 70 °C for 2 h. The slurries were filtrated and washed with excess distilled water, then dried and calcined under the same conditions as above.

CuO/SiO₂, ZnO/SiO₂ and Ag/SiO₂ catalysts were prepared by the conventional wetness impregnation method. Typically, SiO₂ (Qingdao Ocean Chemical Co. Ltd.) support was impregnated with an aqueous solution of Cu(NO₃)₂·3H₂O (Tianjin Damao Chemical Factory, 99.5%), Zn(NO₃)₂·6H₂O (Tianjin Damao Chemical Factory, 99.0%) and AgNO₃ (Tianjin Kemiou Chemical Reagent Co. Ltd., 99.8%), respectively. The loading amount of Cu, Zn and Ag was 3 wt%, 17.2 wt% and 3 wt%, respectively. Then, the obtained materials were dried at 110 °C overnight and calcined in air at 600 °C for 6 h.

Sodium borate (Na₂B₄O₇) was prepared by drying Na₂B₄O₇·10H₂O (Tianjin Damao Chemical Factory, 99.5%) from 60 °C to 120 °C under vacuum. Then, the dehydrated sample was calcined in air at 600 °C for 6 h

Hexagonal boron nitride (h-BN) and anhydrous sodium carbonate (Na_2CO_3) were supplied from Aladdin and Tianjin Kemiou Chemical Reagent Co. Ltd., respectively.

 Na_2CO_3/C was prepared following the reported method [20]. The activated carbon with BET surface area 1365 m^2/g was supplied from Fujian Xinsen Carbon Co. Ltd.. The mass ratio of Na_2CO_3 to C was 9:1.

All composite catalysts were prepared by grinding the mixture containing CsX zeolites and second active component powders in an agate mortar for 30 min, the mass ratio of which was 10:1. The obtained samples were donated as M-CsX-n where M represents the second active components and n represents a or b. For example, $CuO/SiO_2-CsX-a$ indicates a catalyst containing CsX-a and CuO/SiO_2 .

For preparation of granule-stacking sample $Na_2B_4O_7$ -CsX, 40–60 mesh particles of the two components were mixed by shaking in a vessel. Similarly, the dual bed sample $Na_2B_4O_7$ CsX was prepared by separating the granules of the two components with quartz wool.

2.2. Catalyst characterization

The experimental conditions of XRD, SEM, N_2 adsorption–desorption, XPS, NH $_3$ -TPD and CO $_2$ -TPD were in accordance with our previous paper[21].

Toluene-TPD experiment was conducted as follows: the sample (100 mg) was degassed at 450 °C under a flow of helium for one hour. Then, helium gas carrying saturated toluene vapor at 85 °C flowed through the sample at 200 °C for 1 h. Subsequently, a flow of helium purged the sample to remove weakly adsorbed toluene at the same temperature for 1 h. The signal of desorbed toluene was detected with an online mass spectrometer (OmniStar 300, Pfeiffer Vacuum) while temperature increased up to 500 °C (10 °C min $^{-1}$) under a He flow (20 cm 3 min $^{-1}$).

FT-IR spectra of adsorbed methanol were conducted by a Bruker tensor 27 instrument with a resolution of 4 cm $^{-1}$. The powder sample was pressed into thin wafers and then placed into an IR cell equipped with a vacuum system. The sample was activated under vacuum $(10^{\text{-}2}\,\text{pa})$ at 450 °C for 1 h and then exposed to methanol vapor for 3 min at 350 °C. Excess methanol vapor in IR cell was evacuated in the process of temperature dropping to 25 °C. Subsequently, the sample was heated again to 350 °C and further to 430 °C for 30 min without evacuation of IR cell. When the temperature fell back to the room temperature, the corresponding IR spectra were collected.

The retained coke species were analyzed by the Guisnet method [22]. Firstly, the spent catalysts (20 mg) were dissolved in 1.0 ml of 20% HF aqueous solution in a Teflon screwcap. Then 1.0 ml CH_2Cl_2 was slowly added to extract the soluble "coke" species. These organic molecules were analyzed by the GC–MS method that was carried out on an Agilent 7890A gas chromatograph equipped with a HP-5 capillary column (30 m, 0.25 mm i.d., stationary phase thickness 0.25 um) and a mass spectrometer.

A VARIAN Cary-5000 UV-vis-NIR spectrophotometer equipped with an integration sphere in the range of 200–800 nm was applied to record the Ultraviolet-visible (UV-vis) spectrum of the spent catalyst.

2.3. Catalytic testing

The reaction of toluene with methanol was carried out in a quartz reactor on a fixed bed at ambient pressure. The sample (approximately 0.3 g, 40–60 mesh) was loaded and activated in situ at 500 $^{\circ}\text{C}$ under a N_2 flow for 1 h. Then the bed temperature was adjusted to the corresponding reaction temperature.

A liquid mixture of toluene and methanol with a molar ratio varying from 6:1 to 1:1 was pumped steadily into the gasification stove (250 °C) with flowing helium at 10 ml/min and then the mixed stream from the outlet of gasification stove flowed with carrier gas helium through catalyst bed. The effluent products were analyzed by the online gas chromatography (Agilent Technologies GC7890B) equipped with two flame ionization detectors (FID) and one thermal conductivity detector (TCD). A HP-PLOT/Q capillary column (30 m length, diameter 0.53 mm, film thickness 40 um) was connected to one of the FID in order to analyze light products such as methane, ethane and methanol etc. The other FID equipped with a HP-FFAP capillary column (50 m length, diameter 0.32 mm, film thickness 0.5 um) was taken to analyze heavy hydrocarbon such as toluene, xylene and styrene etc. Besides, A TDX-01 $(2 \text{ m} \times 1/8 \text{ "})$ stainless steel packed column was connected to the TCD for analyzing H2, CO and CO2. Both FIDs could detect toluene which served as an internal standard for light and heavy hydrocarbon. Methane could act as an internal standard for CO, CO2 and hydrocarbon as its signal peak appeared in both HP- PLOT/Q capillary column and TDX-01 packed column.

The conversions of toluene (C_T) and methanol (C_M), the aromatics selectivity of styrene and ethylbenzene (S_i), the yields (Y_i), decomposition ratio of methanol and product selectivity (C%) are defined as follows:

$$\begin{split} C_{T}(\%) &= \frac{\sum yi, o}{yTol, o + \sum yi, o} \times 100\% \ . C_{M} \\ &= \frac{\textit{methanol}_{inlet} - \textit{methanol}_{outlet} - 2*\textit{DME}_{outlet}}{\textit{methanol}_{inlet}} \times 100\% \end{split}$$

$$S_i(\%) = \frac{yi, o}{\sum yi, o} \times 100\%. Y_i(\%) = C_T * S_i$$

Product selectivity(C%) = target product_{out}/ Σ product_{out} × 100% Decomposition ratio of methanol= $\frac{CO_{out}+CO2_{out}}{Methanol_{in}}$ × 100%

Where $\sum y_{i,o}$ and $y_{Tol,o}$ are the total molar fractions of aromatic products and the molar fraction of toluene in the outlet, respectively.

3. Results and discussion

 N_2 adsorption–desorption isotherms of all composite samples were shown in Fig. S1. When CsX zeolites were modified by second additives, BET surface area ($S_{\rm BET}$) and micropore volume ($V_{\rm micro}$) decreased to some extent (Table S1). The catalytic performance of all composite samples were examined. The reaction results showed that $Na_2B_4O_7$ was the most effective additive, although the role of these second components was to convert methanol to formaldehyde identically (except for h-BN) (see details in Fig. S2).

3.1. Effects of the properties of CsX in composite catalyst

The composite catalysts were composed of CsX zeolites and second active component, in which CsX was the main active sites for side-chain methylation of toluene. Therefore, the overall activity of composite catalysts would be influenced by the properties of CsX that was affected by the occupancy status, location, and loading capacity of Cs species on zeolites[23–25]. Hence, two types of CsX (CsX-a and CsX-b) were prepared to investigate the effects of the nature of cesium species in the composite catalyst Na₂B₄O₇-CsX on alkylation reactivity.

The alkylation reactivity results on CsX-a and CsX-b were listed in Table 1. Compared to CsX-a, CsX-b exhibited higher styrene (ST) selectivity and the ST to ethylbenzene (EB) ratio as well as lower decomposition ratio of methanol, albeit with a little lower conversion of reactants. The different catalytic performances between CsX-a and CsX-b were not caused by the variation of cesium contents, as confirmed by the comparable Si/Al ratio and Cs/Al ratio for the two samples obtained by XRF analysis (Table 1).

The NH₃-TPD and $\rm CO_2$ -TPD curves of CsX-a and CsX-b were shown in Fig. S3. The number of acid sites on CsX-a was a little less than that on CsX-b, and conversely, the number of base sites on CsX-a was a little

more according to the desorption peak area of NH_3 and CO_2 . The higher base density of CsX-a explains for its higher conversion of reactants.

Furthermore, XPS was employed to confirm the chemical state of Cs species on the zeolite surface (see Fig. S4). Each main peak of cesium $3d_{5/2}$ binding energy could be fitted into two-sub peaks, which indicated that two chemical states of cesium existed. According to the NIST XPS Database[26], the signal of Cs $3d_{5/2}$ near 724 eV belongs to the cesium ion, and the other signal near 725 eV can be assigned to Cs₂O. From Fig. S4, it could be seen that cesium species mainly existed in the form of cesium cations on CsX-b while in the form of Cs₂O on CsX-a, accounting for the higher base density of CsX-a and the higher methanol conversion and decomposition ratio. More ionic cesium species on CsX-b contributes to the higher styrene selectivity.

Next, we compared the reaction reactivity of composite catalysts between Na₂B₄O₇-CsX-a and Na₂B₄O₇-CsX-b (Table 2). The conversions of toluene and methanol on Na₂B₄O₇-CsX-a were a little higher than that on Na₂B₄O₇-CsX-b, the trend of which was the same as the results on CsX-a and CsX-b. However, the ST/EB is 5.15 on Na₂B₄O₇-CsX-b, much higher than that on Na₂B₄O₇-CsX-a. The ST yield on Na₂B₄O₇-CsX-b was also a little higher than its counterpart. The significant difference of catalytic performance between Na₂B₄O₇-CsX-a and Na₂B₄O₇-CsX-b stems from the difference between CsX-a and CsX-b, where the proportion of ionic cesium on CsX-b is higher than that on CsX-a as discussed in the above analysis, which would result in the huge difference in styrene selectivity directly. Therefore, choosing suitable CsX to combine with Na₂B₄O₇ is crucial for the production of styrene.

3.2. Discussion for the reaction mechanism

Although the role of second additive was to convert methanol to formaldehyde identically, $Na_2B_4O_7$ was the most effective one. However, the side chain methylation reactions on our composite catalysts were conducted at 430 °C, which was much lower than the reported temperature (usually higher than 600 °C) for methanol dehydrogenation to formaldehyde including $Na_2B_4O_7[27,28]$. Qiao Han et al.[17] argued that the reaction of toluene with formaldehyde could drive the conversion of methanol to formaldehyde thermodynamically but did not explain why $Na_2B_4O_7$ was superior to other methanol dehydrogenation components in detail. Herein, we confirmed the promoting activity resulting from the formation of formaldehyde induced by $Na_2B_4O_7$ to some extent from our IR experiment of methanol adsorption. Fig. 1 showed the FT-IR spectra of adsorbed methanol on CsX-*b* and $Na_2B_4O_7$ CsX-*b*. When CsX-*b* was exposed to methanol for 3 min at 350 °C, the weak bands at 1614 and 1343 cm⁻¹ were observed as shown in Fig. 1(a),

Table 1 Si/Al and Cs/Al ratios and reaction results on CsX-a and CsX-b.

Sample	Elemental composition ^a		Toluene conv. (%)	Methanol conv. (%)	Methanol decomposition (%)	nanol decomposition (%) Aromatics distribution (%) b		(%) ^b
	Si/Al	Cs/Al				ST	EB	ST/EB
CsX-a	1.14	0.65	2.05	50.36	42.97	52.64	41.51	1.27
CsX-b	1.10	0.68	1.89	43.92	35.37	66.98	24.38	2.75

^a Determined by XRF.

Table 2 The reaction results on Na₂B₄O₇-CsX-a and Na₂B₄O₇-CsX-b.

Sample	Toluene conv. (%)	Methanol conv. (%)	Aromatics distribution (%)		Yield (%)	
			ST	EB	ST	ST/EB
Na ₂ B ₄ O ₇ - CsX-a	8.25	58.15	63.60	33.11	5.24	1.92
Na ₂ B ₄ O ₇ - CsX-b	7.17	47.64	81.55	15.82	5.85	5.15

Data was collected at 33 min time-on-stream. toluene/methanol = 3 (mol ratio); 430 °C; WHSV = $2\ h^{-1}$; He flow: 10 ml/min; Na₂B₄O₇: CsX = 1:10 (wt %).

b Data was collected at 33 min time-on-stream. toluene/methanol = 3 (mol ratio); 430 °C; WHSV = 2 h⁻¹; He flow: 10 ml/min.

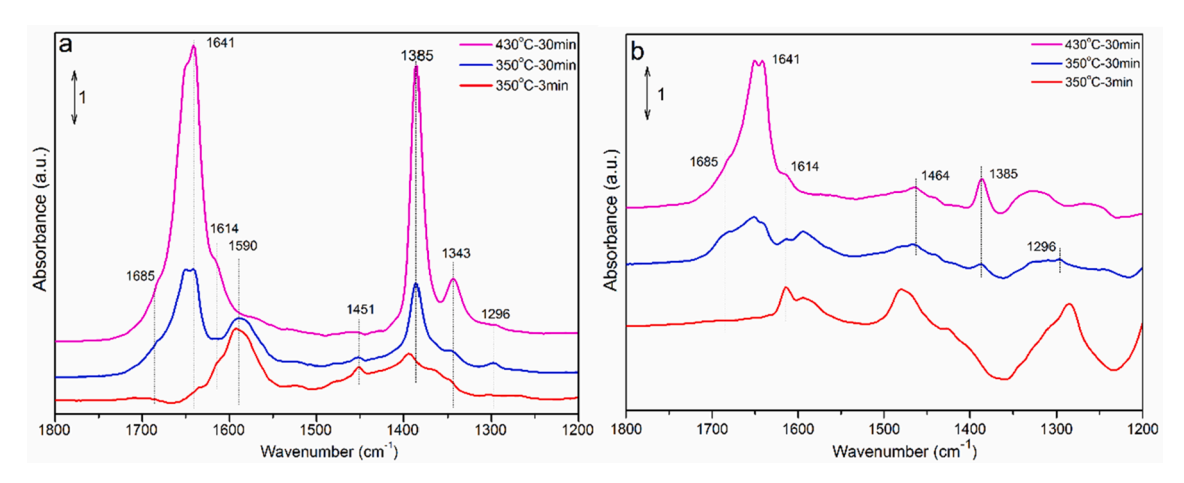


Fig. 1. IR spectra of adsorbed methanol on CsX-b (a), on Na₂B₄O₇-CsX-b (b) after exposure to methanol at 350 °C for 3 min, 30 min and at 430 °C for 30 min, respectively.

which were assigned to bidentate formate [29]. However, the strong bands at 1641 and 1385 cm⁻¹ (assigned to bidentate carbonate) appeared when prolonging heating for 30 min at 350 °C [15]. Meanwhile, the bands at 1685 and 1296 cm⁻¹ could be also observed which were assigned to unidentate formate [29]. The structures of these three adsorbed species were depicted in **scheme S1**. Some researchers suggested that unidentate formate correlated with the side-chain alkylation reaction and its surface concentration was directly proportional to the concentration of formaldehyde in gas phase [15,29,30]. When the temperature increased to 430 °C, the intensities of the bands assigned to bidentate carbonate developed strongly, indicating the decomposition of a large amount of methanol, which was consistent with our reaction results. The band at 1451 cm⁻¹ was related to unreacted methanol and its intensity decreased with the increase of temperature [31].

In contrast, when Na₂B₄O₇-CsX-b was exposed to methanol for 30 min at 350 °C, much more unidentate formate was formed as evidenced by the stronger bands at 1685 and 1296 cm⁻¹ relative to CsX-b, indicating the facile formation of formaldehyde on Na₂B₄O₇-CsX-b. The bands at 1641 and 1385 cm⁻¹ ascribed to bidentate carbonate also appeared and their intensities increased on exposure to methanol at 430 °C for 30 min. However, the intensity ratio of the band at 1685 cm⁻¹ to the band at 1641 cm^{-1} was much higher on Na₂B₄O₇-CsX-b than that on CsX-b, which also suggested that Na₂B₄O₇ was an effective additive for converting methanol to formaldehyde. This result was consistent with the increased base sites when CsX-b modified with Na₂B₄O₇ (see CO₂-TPD in Fig. S3). Furthermore, some active sites for the decomposition of methanol might be covered by sodium borate species, which also resulted in the decreased intensities of the bands assigned to bidentate carbonate. The IR comparison between Na₂B₄O₇-CsX-a and Na₂B₄O₇-CsX-b after adsorbing methanol was shown in Fig. S5. Because more cesium oxide species existed on CsX-a which would contribute to the decomposition of methanol, the higher intensity of the bands at 1641 cm⁻¹ and 1385 cm⁻¹ was observed on Na₂B₄O₇-CsX-a in comparison with that of Na₂B₄O₇-CsX-b.

Other additives also favored the formation of formaldehyde [20,27,28,32]. Therefore, there must be other reasons responsible for the superiority of Na₂B₄O₇. The earlier report suggested that the added boron species as Lewis acidic sites had strong capability of stabilizing toluene, thus resulting in an enhanced alkylation reactivity [16]. However, on our catalyst Na₂B₄O₇-CsX-*b*, both the desorption temperature and the amount of desorbed toluene decreased compared to that of CsX-*b* as shown by the toluene TPD profiles in Fig. 2, although the introduced Na₂B₄O₇ brings about some Lewis acidic sites with medium strength (centered at 270 °C, see NH₃-TPD in Fig. S3). Zhang *et al.* reported a similar result which suggested that introducing some new Lewis acidic sites (FeO_x species) into CsX could reduce the adsorption capability of

toluene [33]. From the results of toluene TPD, we speculated that under our reaction conditions the promotional effect of $Na_2B_4O_7$ did not result from the strong capabilities of stabilizing toluene induced by boron species.

Notedly, Boron species was reported to play a key role in the directed C-H bond activation [34,35]. For example, Fontaine and co-workers described a FLP-catalysed C-H borylation of indoles at the most electron-rich C3 position [34]. Besides, Barluenga et al. reported a basemediated alkylation reaction between tosylhydrazones and boronic acids which provided a C(sp²)-C(sp³) coupling method for the creation of C-C bonds [36]. According to the mechanism of the side chain alkylation of toluene [3,7], the C-H bond in the methyl group of toluene was activated by Lewis base sites, thus the methyl carbon carrying partial negative charge. This carbon with rich electron density was more likely to be attacked by boron with deficient electron, then site-selective C-H borylation of toluene was achieved. Meanwhile, the carbon in formaldehyde has a sp²-hybridized structure with partial positive charge. The carbon(sp³)-carbon(sp²) bond-forming coupling between toluene and formaldehyde completed with the aid of basicity of zeolites. The reaction mechanism was shown in scheme 1. The important role of boron species in the reaction was to construct frustrated Lewis pairs (FLPs) with the base sites on the zeolites. This kind of FLPs activates C-H bond more efficiently and thus improving the performance of the reaction. Furthermore, from the reaction results on BN-CsX (shown in Fig. S2), it could be speculated that the role of other boron additive

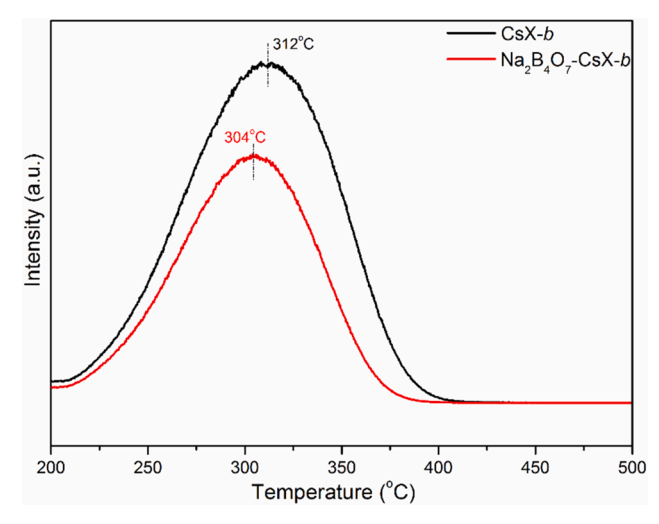


Fig. 2. Toluene TPD profiles of CsX-b and Na₂B₄O₇-CsX-b samples.

species could also be elucidated by this mechanism moderately.

3.3. Effects of integrating manner of Na₂B₄O₇ and CsX

Fig. 3 showed the effects of integrating manner of Na₂B₄O₇ and CsX on side-chain methylation of toluene. It could be seen that the reaction was markedly affected by the mixing mode of two components. By companying with the spatial distance between Na₂B₄O₇ and CsX increasing as the integrating method changed from mortar mixing to dual bed, the toluene conversion (C_T) gradually decreased as shown in Fig. 3(a). Especially for the case of dual bed catalysts, namely the two components were separated by quartz wool, the promoting effect of Na₂B₄O₇ was not obvious. The methanol conversion (C_M) on mortarmixing sample was also highest which was consistent with the C_T as shown in Fig. 3(b). However, the change trend of the C_M with the distance increasing was not monotonous. Moreover, the C_M on dual-bed sample was almost the same as that on CsX, indicating the far distance between the two active components would weaken the coupling effect of the two components. The lowest C_M was achieved on granule-stacking sample. It could also be observed that the C_M decreased with time on stream on the samples with any mixing mode.

The selectivity of side-chain products in aromatics was shown in Fig. 3 (c). The total selectivity of styrene plus ethylbenzene on all samples was close to each other and was more than 90%. However, the styrene selectivity (S_{ST}) was apparently different. The highest S_{ST} was obtained on the granule-stacking sample. Fortunately, the S_{ST} was relatively high on mortar-mixing sample accompanied by the highest conversion of toluene.

The decomposition (to CO and CO₂) ratio of methanol was displayed in Fig. 3 (d). Either mortar-mixing or granule-stacking mode between $\rm Na_2B_4O_7$ and CsX would reduce the decomposition of methanol compared with the results on parent CsX. The lowest ratio was obtained on the granule-stacking sample. As mentioned above, when the $\rm Na_2B_4O_7$ and CsX were separated by quartz wool, the coupling effect would be weakened, which could also be reflected by the decomposition of methanol.

The total yield of styrene plus ethylbenzene and the yield of styrene were shown in Fig. 3(e) and Fig. 3(f), respectively. The highest yields were obtained on the mortar-mixing sample, indicating the closer the distance between $Na_2B_4O_7$ and CsX, the better the catalytic performance for production of styrene. This closer distance between the two components helps to construct frustrated Lewis pairs (FLPs), which supported our proposed mechanism mentioned above.

3.4. Effects of $Na_2B_4O_7$ content on catalytic performance

As discussed above, CsX-b was more suitable than CsX-a to combine with Na₂B₄O₇ for styrene production. Hence, the effects of the amount of Na₂B₄O₇ added to CsX-b were investigated on the sample Na₂B₄O₇-CsXb. Fig. 4 showed the variations of C_T and C_M, the product distribution in aromatics, the ST/EB and styrene yield as a function of Na₂B₄O₇ content in the composite catalyst. The C_T and C_M showed a "volcanic" trend with the increasing of Na₂B₄O₇ content either at the initial or later stage of the reaction (Fig. 4(a)&(c)). The maximum conversion of reactants with time-on-stream varied with Na₂B₄O₇ content. At the initial stage of the reaction (approximately 3 min), the ST/EB was up to 10.02 accompanied with 9.57% conversion of toluene on the Na₂B₄O₇-CsX-b containing 9.09% weight percent of Na₂B₄O₇ (Fig. 4(a)&(b)). The yield of styrene also achieved up to 8.58% (Fig. 4 (b)). However, at the later stage of the reaction, the maximum value of ST/EB and styrene yield were achieved on the sample containing 4.76% weight percent of Na₂B₄O₇ (Fig. 4(d)). It could be observed that the ST/EB maintained a high level more than 7 with time on stream from 3 min to 33 min as well as the yield of styrene maintained approximately 7% on the sample Na₂B₄O₇-CsX-b with 4.76% weight percent of Na₂B₄O₇ (Fig. 4(b)&(d)), indicating that the low content of Na₂B₄O₇ in the composite catalysts was more suitable for the

stability of catalyst. The initial space–time yield of styrene was shown in Fig. S6. A "volcanic" trend with the increasing of $\rm Na_2B_4O_7$ content could also be observed.

Although $Na_2B_4O_7$ could enhance the reaction activity, the main active sites for side-chain methylation of toluene existed in CsX zeolites. When the content of second additive exceeded a certain value, the main active sites decreased even more thus resulting in the decreased reactivity as shown by the "volcanic" trend. Besides, the amount of generated formaldehyde increased with the increasing of added amount of $Na_2B_4O_7$. However, the catalyst was more likely to be deactivated due to higher concentration of formaldehyde in the system [16]. Therefore, the low content of $Na_2B_4O_7$ would be neccessary for the stability of catalyst.

3.5. Effects of Na₂B₄O₇ addition on the properties of catalysts

3.5.1. XRD and SEM

The XRD patterns of CsX-b and Na₂B₄O₇-CsX-b were displayed in Fig. S7. It could be observed that both of them exhibited the characteristic peaks of a faujasite framework [37]. No other diffraction peaks were detected on the Na₂B₄O₇-CsX-b, indicating the Na₂B₄O₇ species were highly dispersed. The SEM images of these two samples were shown in Fig. S8. A morphology of octahedron could be observed from CsX-b with the crystal size of 2–3 μ m. However, much smaller particles adhere to CsX particles appeared in the images of Na₂B₄O₇-CsX-b, which could be assigned to Na₂B₄O₇. The physical mixing of Na₂B₄O₇ and CsX would not change the structure of CsX zeolites, which was indicated by the XRD and SEM results.

3.5.2. The acidity and basicity from IR study

In addition to NH₃-TPD and CO₂-TPD characterization as shown in **Fig. S3**, pyridine and CO₂ adsorption FT-IR experiments were carried out to investigate the acid-base properties of the catalysts. IR spectra of adsorbed pyridine were exhibited in **Fig. 5**. No bands located at 1540 cm⁻¹ could be found on both CsX-*b* and Na₂B₄O₇-CsX-*b* catalysts, indicating that no Brönsted acidic sites existed on both samples [38]. The bands at 1580 cm⁻¹ and 1440 cm⁻¹ were assigned to Lewis acidic sites [14,39]. It could be observed that the peak intensity of the band at 1580 cm⁻¹ decreased and the band at 1440 cm⁻¹ even disappeared by evacuation at 150 °C when CsX zeolites were modified by sodium borate (**Fig. 5 a & c**), indicating that the amount of acid sites decreased after modification with sodium borate. With the evacuation temperature increasing to 250 °C, the intensity of all bands decreased obviously, suggesting the strength of acid sites was not so strong (**Fig. 5 b & d**).

Fig. 6 showed the IR spectra of the adsorption of CO_2 on the catalysts. It was reported that some carbonate-like species would be formed by interacting of CO_2 with basic centers on the zeolites, which would produce characteristic IR bands in the range of 1800-1300 cm $^{-1}$ [40–42]. As shown in Fig. 6, a pair of bands centered at 1645 and 1381 cm $^{-1}$ were observed on both CsX-b and $Na_2B_4O_7$ -CsX-b evacuated at $100\,^{\circ}$ C (Fig. 6 a & c), which was assigned to carbonates formed by the reaction of CO_2 with basic zeolite oxygen atoms [43,44]. The band intensity was slightly weaker for CsX-b than for $Na_2B_4O_7$ -CsX-b, indicating the basic sites increased a little by modification with sodium borate. With the evacuation temperature increasing to $250\,^{\circ}$ C, these bands almost disappeared (Fig. 6 b & d). These results were in line with the results of CO_2 -TPD.

3.6. Effects of reaction conditions

The various reaction conditions including toluene/methanol mole ratio, temperature and space velocities were investigated using $Na_2B_4O_7$ -CsX-b as a catalyst. From Fig. 7a, it could be seen that the C_M increased monotonically with the temperature increasing while the C_T increased from 370 to 430 °C, and then decreased a little when the temperature was up to 500 °C. Although higher temperature is benefit for methanol conversion to formaldehyde on $Na_2B_4O_7$ [27], the

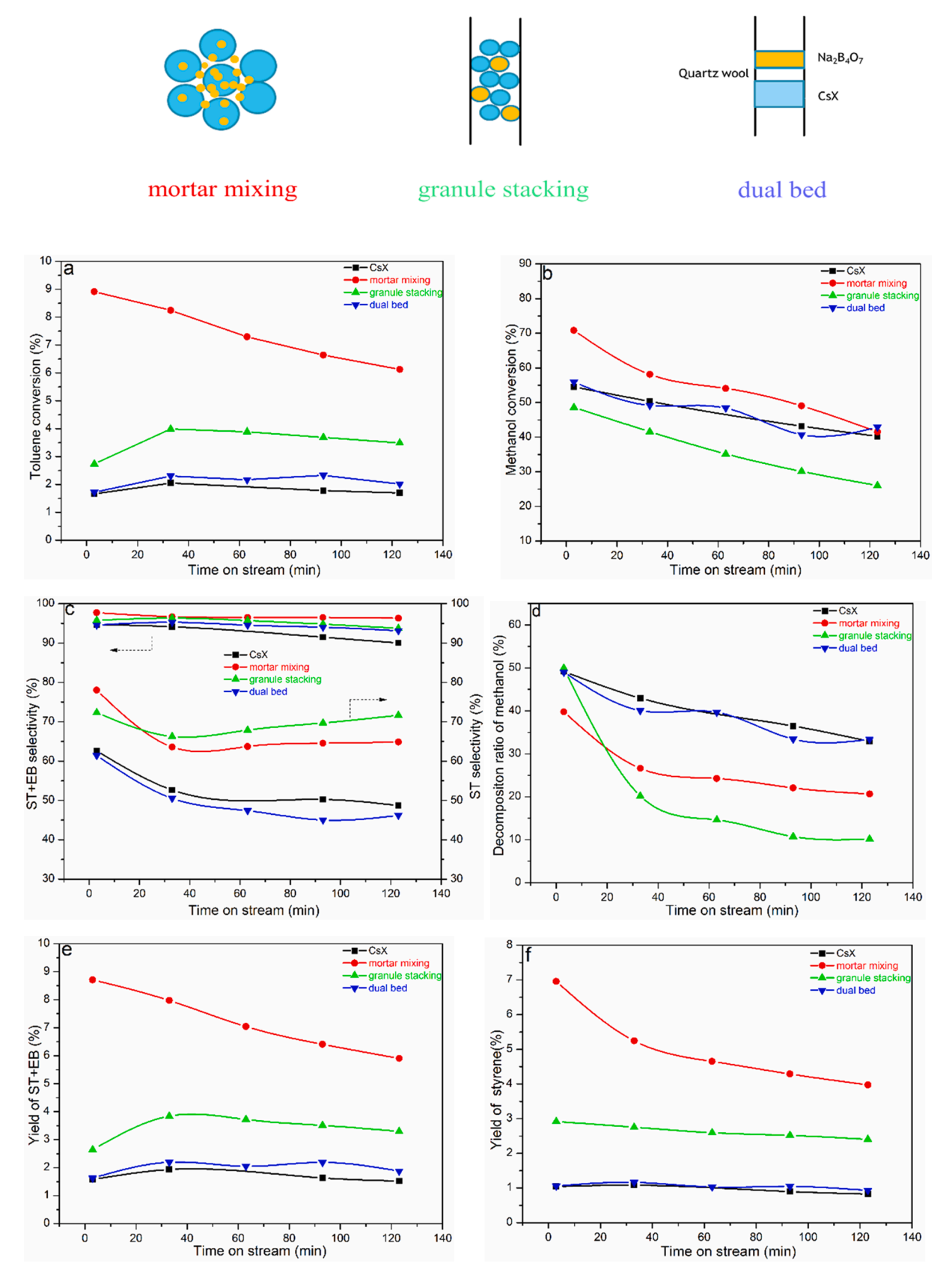


Fig. 3. toluene conversion (a), methanol conversion (b), selectivity of side-chain products in aromatics (c), the decomposition ratio of methanol (d), total yield of styrene and ethylbenzene (e), yield of styrene (f), as a function of time on stream on $Na_2B_4O_7$ -CsX with different integration manner. The CsX used here refers to CsX-a. Reaction conditions: 430 °C, WHSV = 2 h⁻¹, n(toluene)/n(methanol) = 3.

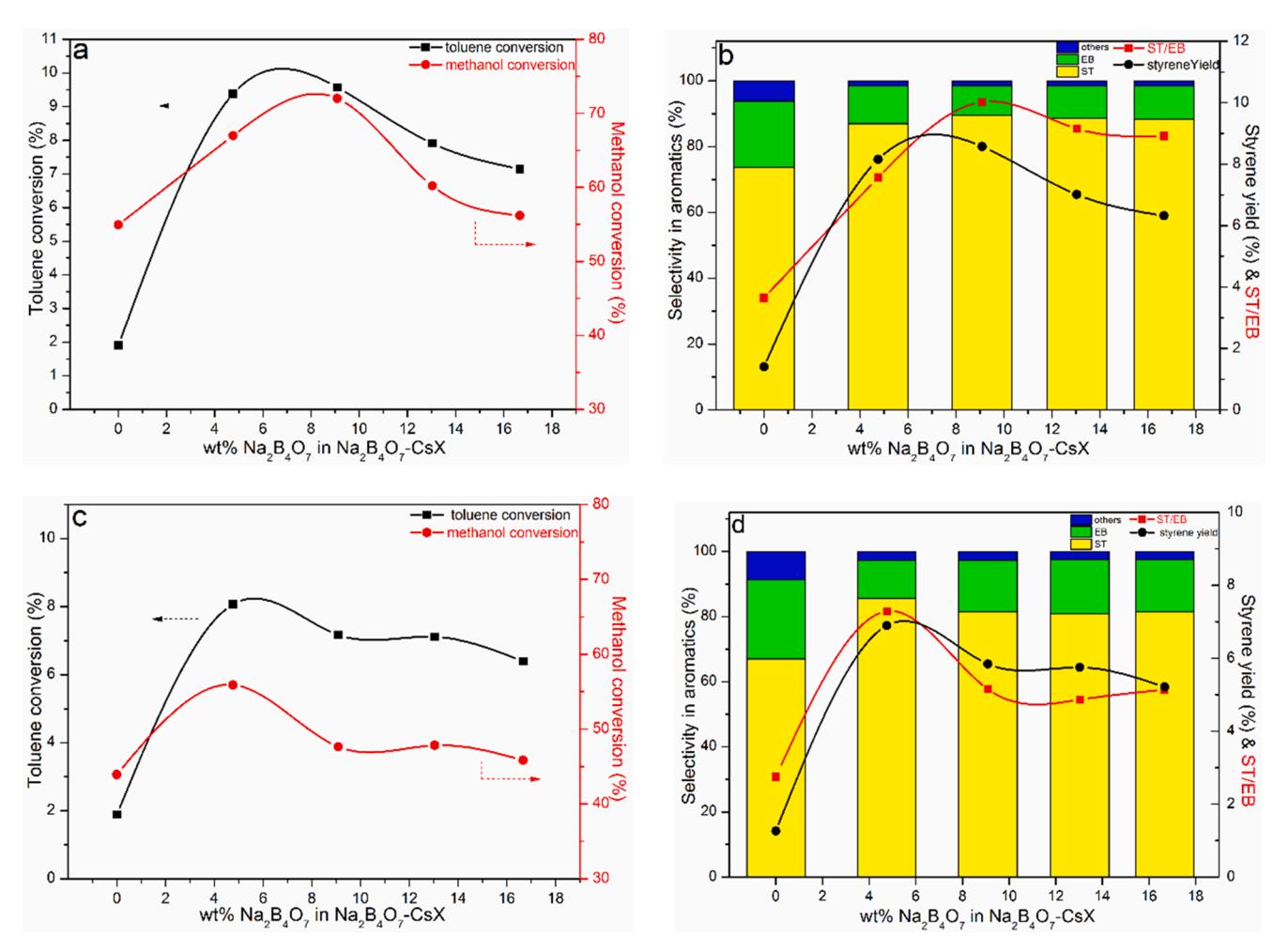


Fig. 4. conversion of toluene and methanol (a)(c), the selectivity in aromatics, the ST/EB and styrene yield (b)(d) as a function of $Na_2B_4O_7$ content in $Na_2B_4O_7$ -CsX-b. (a) & (b) was determined at 3 min while (c) & (d) was determined at 33 min with time on stream. Reaction conditions: 430 °C, WHSV = 2 h⁻¹, n(toluene)/n (methanol) = 3.

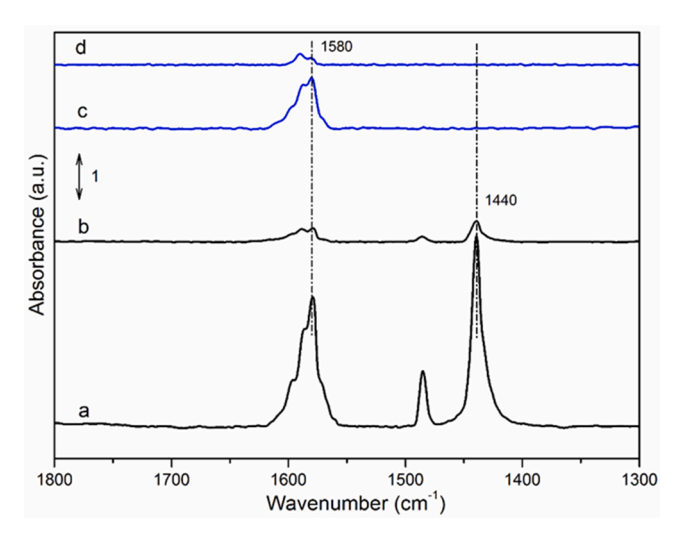


Fig. 5. FT-IR spectra of Py adsorbed on CsX-b (a & b) and Na₂B₄O₇-CsX-b (c & d). a & c evacuated at 150 °C while b & d evacuated at 250 °C.

stabilization of toluene on the catalyst would become difficult. In the product distribution, the $S_{\rm ST}$ decreased with the temperature rising while both ethylbenzene and CO selectivity increased, indicating the self-decomposition of methanol and the secondary hydrogenation of

styrene intensified at higher temperature. Fig. 7b shows the effect of space velocity. Both C_T and C_M decreased with the increasing of space

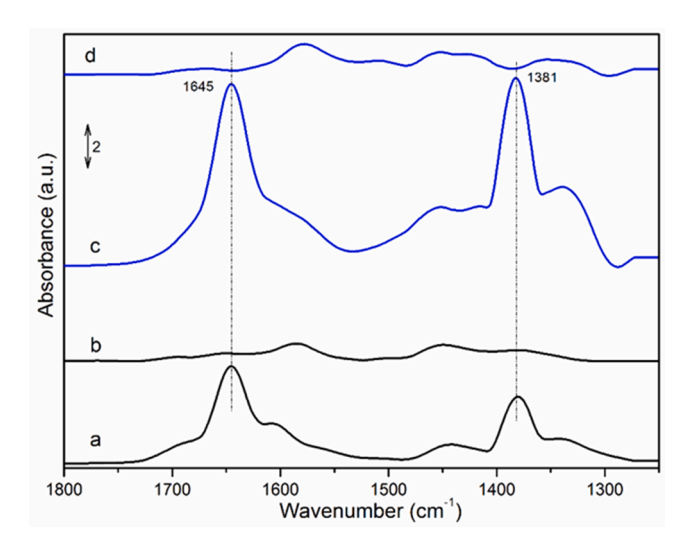


Fig. 6. IR spectra of CO_2 adsorbed on CsX-b (a & b) and $Na_2B_4O_7$ -CsX-b (c & d) under different evacuation temperature. a & c evacuated at 100 °C while b & d evacuated at 250 °C. All spectra had subtracted the corresponding spectrum before CO_2 adsorption.

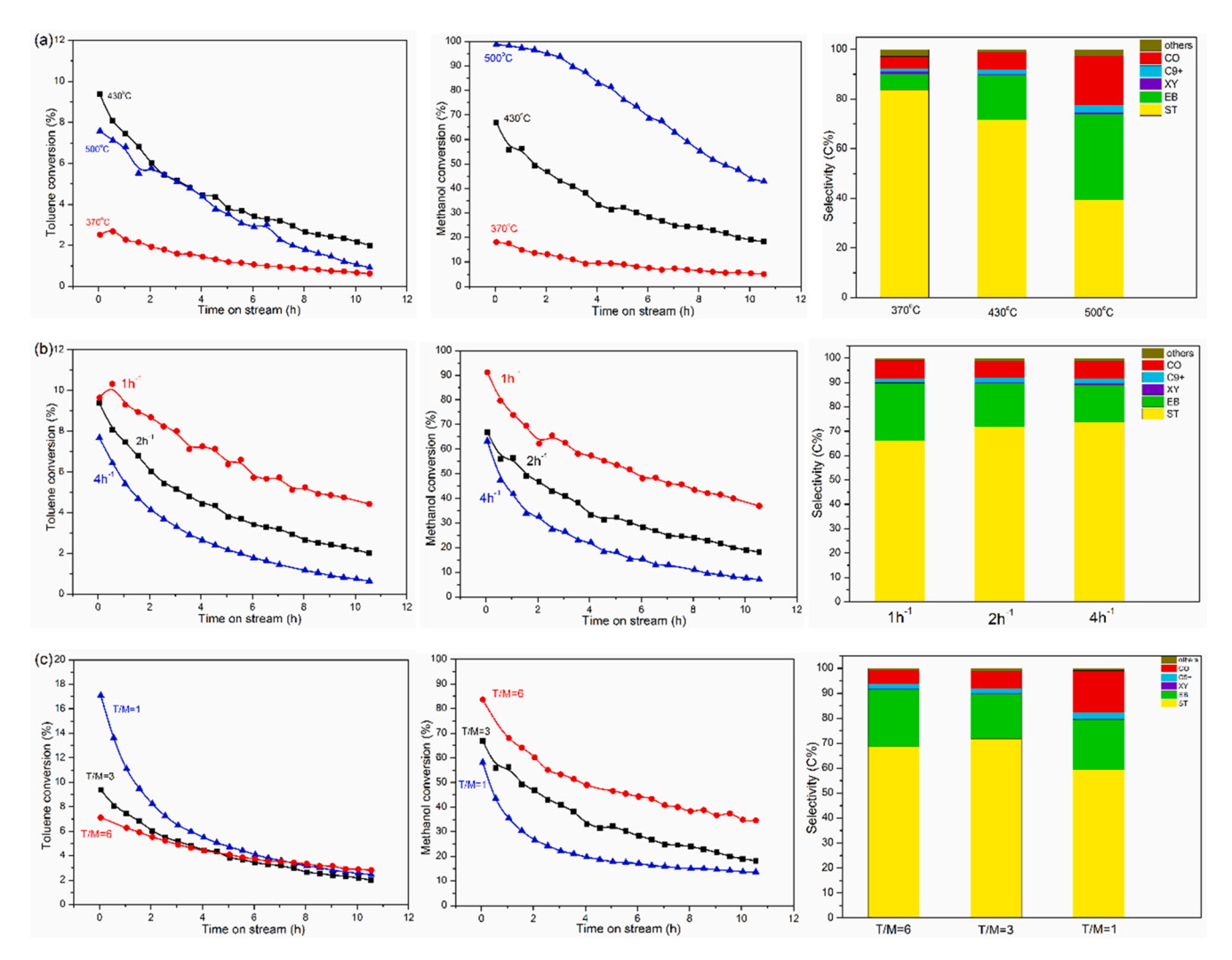


Fig. 7. Catalytic performances of $Na_2B_4O_7$ -CsX-b ($Na_2B_4O_7$: CsX = 1:20 (wt%)) under different reaction conditions: (a) varying reaction temperature with constant toluene/methanol ratio (T/M = 3) and space velocity (WHSV = 2.0 h⁻¹); (b) varying space velocity with constant temperature (430 °C) and toluene/methanol ratio (T/M = 3); (c) varying toluene/methanol ratio with constant temperature and space velocity (WHSV = 2.0 h⁻¹); The selectivity (C%) was determined at 63 min time-on-stream.

velocity while the ST/EB ratio gradually increased. It is not difficult to understand this phenomenon, because styrene is the primary product and short contact time would inhibit the secondary hydrogenation of styrene. The effect of the ratio of toluene to methanol was shown in Fig. 7c. As expected, the C_M increased while C_T decreased with the increasing T/M ratio. However, at the later stage of the reaction, different T/M ratios seemed to have less influence on the conversion of toluene. Even, a little higher conversion of toluene was obtained at the condition of higher T/M ratio. This could be explained by the fact that the catalysts deactivated at the later stage of the reaction and more methanol in the feed was more inclined to result in the deactivation of catalyst. Usually, high T/M ratio (typically T/M greater than 3) was applied to inhibit the decomposition of methanol[9,12,18]. However, from the results of product distribution, it could be observed that CO selectivity under the condition of T/M = 3 is just a little higher than that of T/M=6, which implies CsX modified with $Na_2B_4O_7$ indeed inhibit methanol decomposition. This was consistent with the discussion above. We have also calculated the space-time yield of styrene under different conditions at the beginning of the reaction, as illustrated in Fig. 8. The highest yield was obtained at 430 °C, space velocity of 4 h⁻¹ and T/M ratio of 3. Although higher space velocity was good for styrene production, the conversion of reactants was relatively lower.

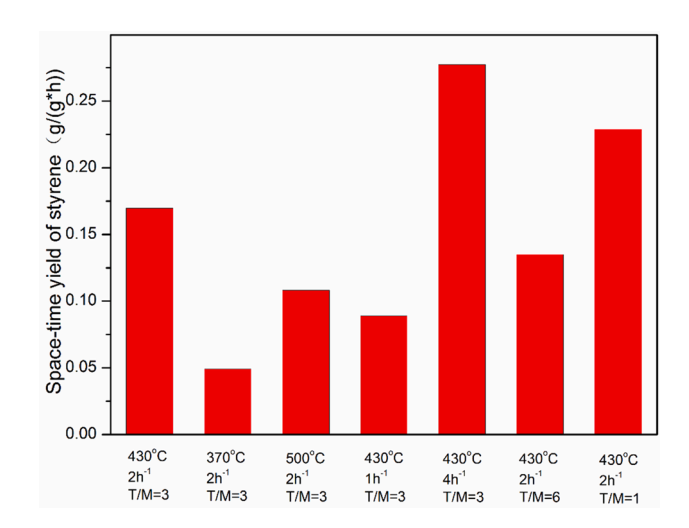


Fig. 8. The space–time yield of styrene under different reaction conditions; Data was collected at 3 min time-on-stream.

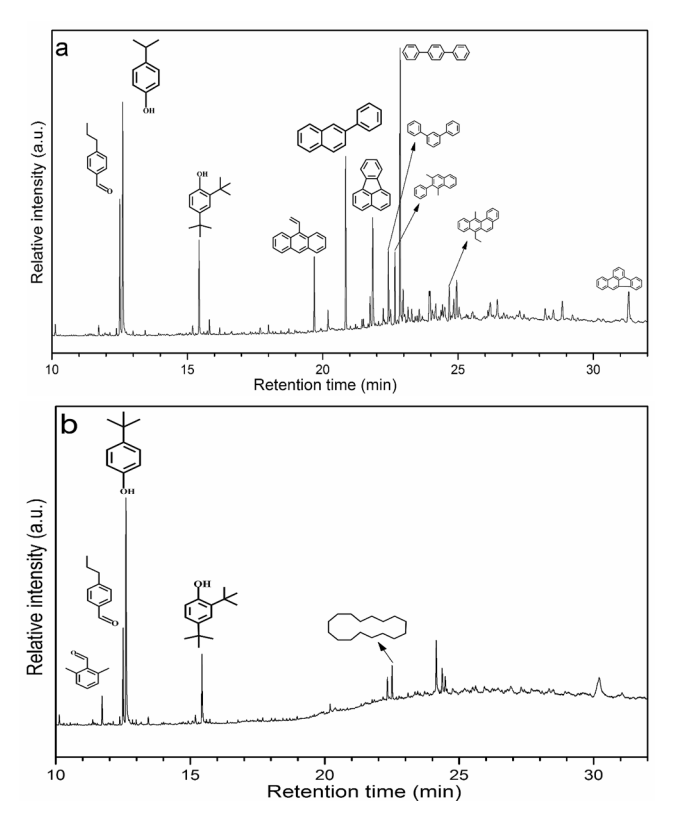


Fig. 9. GC–MS chromatograms of coke species at reaction temperature 430 $^{\circ}$ C (a), 500 $^{\circ}$ C (b) after 11 h retained in Na₂B₄O₇-CsX-b. WHSV = 2 h⁻¹; T/M = 3 (mol ratio).

3.7. The carbon deposition on spent Na₂B₄O₇-CsX-b and regeneration of the catalyst

It could be found that CsX zeolites modified with $Na_2B_4O_7$ tended to be deactivated under various conditions. Therefore, the coke species on spent catalysts were investigated by the GC–MS method, as shown in Fig. 9. It was observed that the confined materials at 430 °C were mainly polycyclic aromatics. Besides, 4- propylbenzaldehydeas well as polyalkylphenol was also detected. At higher reaction temperature (500 °C), the peaks representing polycyclic aromatic hydrocarbons almost disappeared while the peaks attributes to polyalkylphenol and 4-

propylbenzaldehyde still existed and kept relatively high intensity. Noticeably, a new peak appeared at a retention time of 11.7 min representing a new confined oxygenated compound. Although CsX zeolites (FAU-type) have supercages which could accommodate up polycyclic aromatics, these species may go through further hydrogen transfer and cyclization to form larger polycyclic coke species at higher temperature, which would be difficult to be extracted with CH₂Cl₂. This could explain why smaller amounts of coke species were detected at higher reaction temperature. TG curves of the spent catalysts were exhibited in Fig. S9, which supported this speculation. The initial weight loss could be attributed to the desorption of physically adsorbed water and organics (30–300 °C). The other weight loss above 300 °C was ascribed to the decomposition of coke species deposited over the catalysts [23]. The coke amount at reaction temperature 500 °C (8.5%) was higher than that at 430 °C (4.2%), which was in line with the above analysis. UV-vis spectroscopy of the deactivated catalysts also supported this speculation (see Fig. \$10). Large polycyclic coke species block the diffusion path of the reactants and ultimately causing the deactivation of the catalysts.

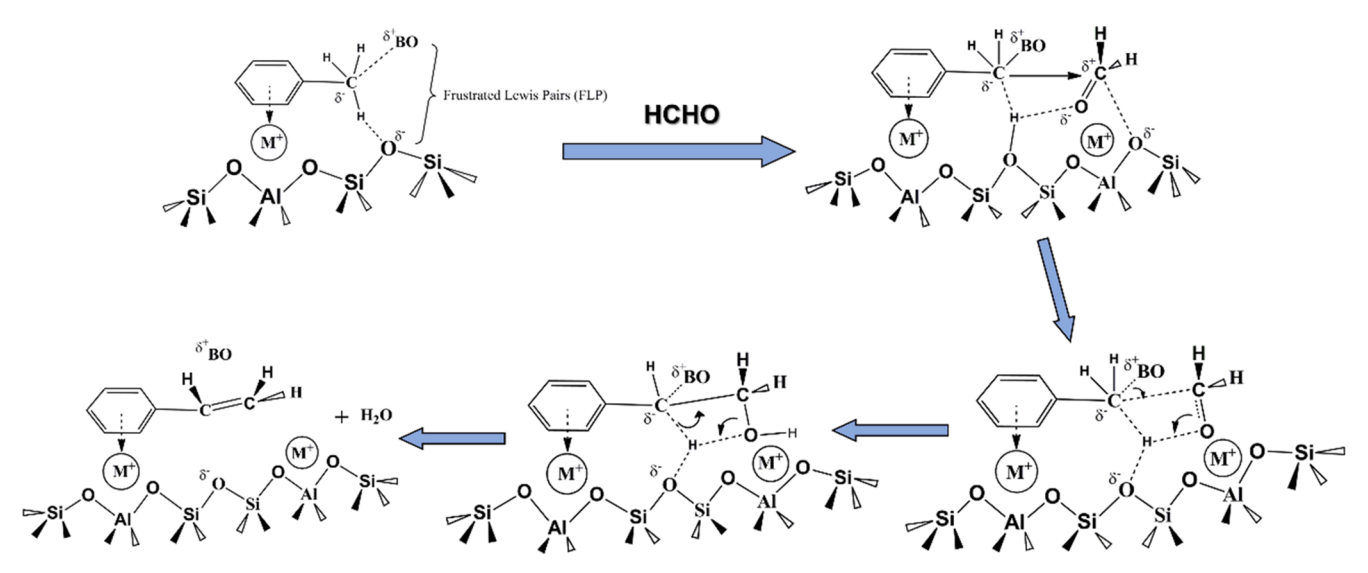
The activity recovered after regeneration of the spent catalysts through coke combustion. The reaction results were shown in Fig. S11. It could be seen that the conversions of reactants were a little higher on the regenerated catalysts. However, the selectivity of styrene decreased while the selectivity of ethylbenzene increased compared with the results on fresh catalyst.

4. Conclusion

 $\rm Na_2B_4O_7$ was found to be an effective additive to promote the reactivity of side-chain methylation and a new synergistic reaction mechanism was proposed to explain the promotion effect of boron additives. The superiority of $\rm Na_2B_4O_7$ lies in two aspects: 1) the addition of $\rm Na_2B_4O_7$ contributes to the formation of the reaction intermediate formaldehyde; 2) boron species adjacent to basic sites on the zeolites construct the frustrated Lewis pairs (FLPs), which could activate C–H bond in the methyl group of toluene more efficiently. Importantly, we speculated that the promotion effect of other boron additives could also be elucidated by this mechanism moderately. By adjusting the mass ratio and the spatial proximity of the two components and tuning the chemical nature of cesium in CsX, a much higher selectivity of styrene along with relatively high conversion of toluene was achieved.

CRediT authorship contribution statement

Qijun Yu: Conceptualization, Methodology, Formal analysis,



Scheme 1. The proposed synergistic reaction mechanism of toluene alkylation with methanol in the presence of added boron species.

Investigation, Writing - original draft, Visualization. Jinzhe Li: Formal analysis, Writing - review & editing. Changcheng Wei: Investigation, Validation. Zhongmin Liu: Conceptualization, Writing - review & editing, Supervision, Project administration.

Declaration of Competing Interest

The authors declare that they have no known competing financial interests or personal relationships that could have appeared to influence the work reported in this paper.

Acknowledgement

We acknowledge the National Natural Science Foundation of China (NO. 21991093 and 21991090) for the financial support.

Appendix A. Supplementary data

Supplementary data to this article can be found online at https://doi.org/10.1016/j.fuel.2020.119270.

References

- [1] Perego C, Ingallina P. Recent advances in the industrial alkylation of aromatics: new catalysts and new processes. Catal Today 2002;73(1–2):3–22.
- [2] Al-Khattaf S, Ali SA, Aitani AM, Žilková N, Kubička D, Čejka J. Recent Advances in Reactions of Alkylbenzenes Over Novel Zeolites: The Effects of Zeolite Structure and Morphology. Cat Rev - Sci Eng 2014;56(4):333–402.
- [3] Itoh H, Miyamoto A, Murakami Y. Mechanism of the Side-Chain Alkylation of Toluene with Methanol. J Catal 1980;64(2):284–94.
- [4] Itoh H, Hattori T, Suzuki K, Murakami Y. Role of Acid and Base Sites in the Side-Chain Alkylation of Alkylbenzenes with Methanol on Two-Ion-Exchanged Zeolites. J Catal 1983;79(1):21–33.
- [5] Borgna A, Sepúlveda J, Magni SI, Apesteguía CR. Active sites in the alkylation of toluene with methanol: a study by selective acid-base poisoning. Appl Catal, A 2004:276(1–2):207–15.
- [6] Anderson MW, Philippou A. Solid-state NMR Investigation of the Alkylation of Toluene with Methanol over Basic Zeolite X. J Am Chem Soc 1994;116(13): 5774–83.
- [7] Palomares AE, Eder-Mirth G, Lercher JA. Selective Alkylation of Toluene over Basic Zeolites: An in Situ Infrared Spectroscopic Investigation. J Catal 1997;168(2): 442–9
- [8] Li P, Han Q, Zhang X, Yuan Y, Zhang Y, Guo H, et al. A new insight into the reaction behaviors of side-chain alkylation of toluene with methanol over CsX. Catal Sci Technol 2018;8(13):3346–56.
- [9] Han H, Liu M, Nie X, Ding F, Wang Y, Li J, et al. The promoting effects of alkali metal oxide in side-chain alkylation of toluene with methanol over basic zeolite X. Microporous Mesoporous Mater 2016;234:61–72.
- [10] Barthomeuf D. Conjugate Acid-Base Pairs in Zeolites. J Phys Chem 1984;88.
- [11] Okamoto Y, Ogawa M, Maezawa A, Imanaka T. Electronic Structure of Zeolites Studied by X-Ray Photoelectron Spectroscopy. J Catal 1988;112(2):427–36.
- [12] Garces JM, Wieland WS, Davis RJ. Side-Chain Alkylation of Toluene with Methanol over Alkali-Exchanged Zeolites X, Y, L, and β. J Catal 1998;173(2):490–500.
- [13] Palomares AE, Eder-Mirth G, Rep M, Lercher JA. Alkylation of Toluene over Basic Catalysts—Key Requirements for Side Chain Alkylation. J Catal 1998;180(1): 56–65
- [14] Tope BB, Alabi WO, Aitani AM, Hattori H, Al-Khattaf SS. Side-chain alkylation of toluene with methanol to styrene over cesium ion-exchanged zeolite X modified with metal borates. Appl Catal, A 2012;443:214–20.
- [15] Hattori H, Amusa AA, Jermy RB, Aitani AM, Al-Khattaf SS. Zinc oxide as efficient additive to cesium ion-exchanged zeolite X catalyst for side-chain alkylation of toluene with methanol. J Mol Catal A: Chem 2016;424:98–105.
- [16] Lee H, Lee S, Ryoo R, Choi M. Revisiting side-chain alkylation of toluene to styrene: Critical role of microporous structures in catalysts. J Catal 2019;373:25–36.
- [17] Han Q, Li P, Zhang Y, Lu P, Xu L, Guo H, et al. Conversion of MeOH and Toluene into Styrene and Ethylbenzene Using Composite Catalysts Containing MeOH Dehydrogenation Components. ChemCatChem 2019;11(6):1610–4.

- [18] Wieland WS, Davis RJ, Garces JM. Solid base catalysts for side-chain alkylation of toluene with methanol. Catal Today 1996;28(4):443–50.
- [19] Martin AJ, Mitchell S, Scholder O, Verel R, Hauert R, Bernard L, et al. Elucidating the Distribution and Speciation of Boron and Cesium in BCsX Zeolite Catalysts for Styrene Production. ChemPhysChem 2018;19(4):437–45.
- [20] Su S, Prairie MR, Renken A. Promoting effect of active carbons on methanol dehydrogenation on sodium carbonate: Hydrogen spillover. Appl Catal, A 1993;95 (1):131–42.
- [21] Yu Q, Li J, Wei C, Zeng S, Xu S, Liu Z. Role of ball milling during Cs/X catalyst preparation and effects on catalytic performance in side-chain alkylation of toluene with methanol. Chinese J Catal 2020;41(8):1268–78.
- [22] Magnoux P, Roger P, Canaff C, Fouche V, Gnep NS, Guisnet M. New Technique for the Characterization of Carbonaceous Compounds Responsible for Zeolite Deactivation. Stud Surf Sci Catal 1987;34:317–30.
- [23] Han H, Liu M, Ding F, Wang Y, Guo X, Song C. Effects of Cesium Ions and Cesium Oxide in Side-Chain Alkylation of Toluene with Methanol over Cesium-Modified Zeolite X. Ind Eng Chem Res 2016;55(7):1849–58.
- [24] Lasperas M, He Cambon, Brunel D, Rodriguez I, Geneste P. Cesium oxide encapsulation in faujasite zeolites effect of framework composition on the nature and basicity of intrazeolitic species. Microporous Mater 1996;7(2):61–72.
- [25] Borgna A, Magni S, Sepúlveda J, Padró CL, Apesteguía CR. Side-chain alkylation of toluene with methanol on Cs-exchanged NaY zeolites: effect of Cs loading. Catal Lett 2005;102(1–2):15–21.
- [26] NIST X-ray Photoelectron Spectroscopy Database. Doi: 10.18434/T4T88K.
- [27] Andreas Meyer AR. Sodium Compounds as Catalysts for Methanol Dehydrogenation to Water-Free Formaldehyde. Chem Eng Technol 1990;13(3): 145-9
- [28] Su S, et al. Catalytic Dehydrogenation of Methanol to Water-Free Formaldehyde. Chem Eng Technol 1994;17(1):34–40.
- [29] King ST, Graces JM. In Situ Infrared Study of Alkylation of Toluene with Methanol on Alkali Cation-Exchanged Zeolites. J Catal 1987;104(1):59–70.
- [30] Unland ML. Infrared Study of Methanol Decomposition on Alkali Metal X-Type Zeolites. J Phys Chem 1978;82(5):580–3.
- [31] Rep M, Palomares AE, Eder-Mirth G, Ommen JGv, Rösch N, Lercher JA. Interaction of Methanol with Alkali Metal Exchanged Molecular Sieves. 1. IR Spectroscopic Study. J Phys Chem B 2000;104(104):8624–30.
- [32] Andreja Music JB. Janez Levec Gas-phase catalytic dehydrogenation of methanol to formaldehyde over ZnO/SiO₂ based catalysts, zeolites, and phosphates. Appl Catal A 1997:165:115–31.
- [33] Zhang Z, Yuan X, Miao S, et al. Effect of Fe Additives on the Catalytic Performance of Ion-Exchanged CsX Zeolites for Side-Chain Alkylation of Toluene with Methanol. Catalysts 2019;9(10).
- [34] Légaré M-A, Courtemanche M-A, Rochette É, Fontaine F-G. Metal-free catalytic C-H bond activation and borylation of heteroarenes. Science 2015;349(6247):513–6.
- [35] Lv J, Chen X, Xue X-S, Zhao B, Liang Y, Wang M, et al. Metal-free directed sp²-C-H borylation. Nature 2019;575(7782):336–40.
- [36] Barluenga J, Tomas-Gamasa M, Aznar F, Valdes C. Metal-free carbon-carbon bondforming reductive coupling between boronic acids and tosylhydrazones. Nat Chem 2009;1(6):494–9.
- [37] Fan F, Feng Z, Li G, Sun K, Ying P, Li C. In situ UV Raman spectroscopic studies on the synthesis mechanism of zeolite X. Chem-A Eur J 2008;14(17):5125–9.
- [38] Ueda R, Kusakari T, Tomishige K, Fujimoto K. Nature of Spilt-over Hydrogen on Acid Sites in Zeolites: Observation of the Behavior of Adsorbed Pyridine on Zeolite Catalysts by Means of FTIR. J Catal 2000;194(1):14–22.
- [39] Jiang J, Lu G, Miao C, Wu X, Wu W, Sun Q. Catalytic performance of X molecular sieve modified by alkali metal ions for the side-chain alkylation of toluene with methanol. Microporous Mesoporous Mater 2013;167:213–20.
- [40] Bisio C, Fajerwerg K, Martra G, Massiani P. Investigation of co-hosted basic and metal nanoparticles in Pt/Cs-BEA zeolites. Catal Today 2007;124(1-2):36-42.
- [41] Galhotra P, Navea JG, Larsen SC, Grassian VH. Carbon dioxide (C¹⁶O₂ and C¹⁸O₂) adsorption in zeolite Y materials: effect of cation, adsorbed water and particle size. Energy Environ Sci 2009;2(4):401–9.
- [42] Jacobs P, Vancauwe FH, Vansatn E. Surface Probing of Synthetic Faujasites by Adsorption of Carbon Dioxide. Part 2. -Infra-red Study of Carbon Dioxide adsorbed on X Zeolites exchanged with Mono- and Bi-valent Ions. J Chem Soc Faraday Trans 1973;69(12):2130–9.
- [43] Martra G, Coluccia S, Davit P, Gianotti E, Marchese L, Tsuji H, et al. Acidic and basic sites in NaX and NaY faujasites investigated by NH₃, CO₂ and CO molecular probes. Res Chem Intermed 1999;25(1):77–93.
- [44] Lavalley JC. Infrared spectrometric studies of the surface basicity of metal oxides and zeolites using adsorbed probe molecules. Catal Today 1996;27(3-4):377-401.